

A Characteristic Dense Environment or Wind Signature in Prompt GRB Afterglows

Shiho Kobayashi^{1,2}, Peter Mészáros^{1,2} and Bing Zhang¹

¹*Department of Astronomy & Astrophysics, Pennsylvania State University, University Park, PA 16802*

²*Center for Gravitational Wave Physics, Pennsylvania State University, University Park, PA 16802*

ABSTRACT

We discuss the effects of synchrotron self-absorption in the prompt emission from the reverse shock of GRB afterglows occurring in a dense environment, such as the wind of a massive stellar progenitor or a dense ISM in early galaxies. We point out that, when synchrotron losses dominate over inverse Compton losses, the higher self-absorption frequency in a dense environment implies a bump in the reverse shock emission spectrum, which can result in a more complex optical/IR light curve than previously thought. This bump is prominent especially if the burst ejecta is highly magnetized. In the opposite case of low magnetization, inverse Compton losses lead to a prompt X-ray flare. These effects give a possible new diagnostic for the magnetic energy density in the fireball, and for the presence of a dense environment.

Subject headings: gamma rays: bursts - shock waves - radiation mechanisms: thermal

1. Introduction

Snapshot fits of the broadband spectrum of gamma-ray burst (GRB) afterglows to standard forward shock models have been found, in many cases, to be consistent with an external environment density $n \lesssim 1 \text{ cm}^{-3}$ typical of a dilute interstellar medium (ISM) which, to first order, can be taken to be approximately independent of distance from the burst (Frail et al 2001). In other cases, the forward shock is better fitted with an external density which depends on distance as $\rho \propto R^{-2}$, typical of a stellar wind environment (Chevalier & Li 1999, 2000; Li & Chevalier 2003). The two types of fits have been critically analyzed by e.g., Panaitescu and Kumar (2002), the conclusion being that at least some bursts may occur in

high mass-loss winds, as expected from massive progenitors. The parameters for such wind fits are uncertain, due to poorly known stellar mass loss rates.

In this Letter we show that observations of prompt optical/IR and/or X-ray emission attributable to reverse shock emission could constraint the GRB environment. The reverse shock emission tends to be in the regime where the electron cooling time is shorter than the dynamical expansion time. In high density environments, such as a stellar progenitor wind or a dense ISM in early galaxies, the self-absorption (SA) frequency is much higher than in the normal ISM, and it could be much higher than the typical injection peak frequency. Here we argue, from general radiative transfer considerations, that in such situations when the emission is in the fast cooling regime and the SA frequency is higher than the injection frequency, the SA frequency and its scaling are different from, and the flux at the SA frequency is appreciably larger than, what had been previously estimated. This implies a different light curve time behavior for the afterglow prompt flash in a dense environment. This is of significant interest, since observations of the SA frequency and the net flux could provide constraints on the otherwise poorly known wind mass-loss rates of progenitors stars, or on the presence of a dense ISM. These new features are expected to be pronounced if the inverse Compton process does not play a dominant role. This could happen in the case of highly magnetized fireball ejecta, whose presence has been suggested by some recent studies (Zhang, Kobayashi & Mészáros 2003; Kumar & Panaiteescu 2003) and by reports of high gamma-ray polarization (Coburn & Boggs 2003). The strength of the SA features would then provide a constraint on the magnetization parameter.

2. The Model

We consider a relativistic shell (fireball ejecta) with an isotropic energy E , an initial Lorentz factor η and an initial width Δ_0 expanding into a surrounding medium with a density distribution $\rho = AR^{-2}$. The shell width Δ_0 is related to the intrinsic duration of the GRB as $\Delta_0 \sim (1+z)^{-1}cT$ (Kobayashi, Piran & Sari 1997) where z is the redshift of the burst. The interaction between the shell and the wind is described by two shocks: a forward shock propagating into the wind and a reverse shock propagating into the shell. The shocks accelerate electrons in the shell and in the wind material, and the electrons emit photons via synchrotron process.

The evolution of the reverse shocks can be classified into two cases depending on the value of the initial bulk Lorentz factor η relative to a critical value $\eta_{cr} = ((1+z)E/4\pi Ac^3T)^{1/4}$ (Sari & Piran 1995; Kobayashi & Zhang 2003b). If $\eta > \eta_{cr}$ (thick-shell case), the reverse shock starts out relativistic and it significantly decelerates the shell material, to

$\Gamma \sim \eta_{cr}$. If $\eta < \eta_{cr}$ (thin-shell case), the reverse shock is initially Newtonian and becomes only mildly relativistic traversing the shell. Most bursts in a wind environment fall in the thick-shell class, ($\eta > \eta_{cr}$), because the high density implies a critical Lorentz factor $\eta_{cr} \sim 70 \zeta^{1/4} E_{53}^{1/4} A_{11.7}^{-1/4} T_{50}^{-1/4}$ lower than the typical value in fireball models $\eta \gtrsim 100$ (e.g., Lithwick & Sari 2001), where $\zeta = (1+z)/2$, $E_{53} = E/10^{53}$ ergs, the duration $T_{50} = T/50$ sec, and $A_{11.7} = A/5 \times 10^{11}$ g cm⁻¹ is a typical wind mass loss rate. We are especially interested in long bursts with $t_x \gtrsim 1$ minute, for the purpose of analyzing the light curve behavior of the reverse shock emission. We focus on the thick-shell case, for which one can take the shock crossing time $t_x \sim T$ and the bulk Lorentz factor during the shock crossing ($t < t_x$) is $\Gamma \sim \eta_{cr}$.

If we neglect synchrotron self-absorption (which is discussed in the next section) the spectrum of the reverse shock is described by a broken power law with a peak $F_{\nu,max}$ and two break frequencies: a typical frequency ν_m and a cooling frequency ν_c (Sari, Piran & Narayan 1998). Assuming that constant fractions (ϵ_e and ϵ_B) of the internal energy produced by the shock go into the electrons and the magnetic field, the reverse shock spectrum at a shock crossing time $t_x \sim T$ is characterized by (Kobayashi & Zhang 2003b),

$$\nu_c(T) \sim 1.5 \times 10^{11} \zeta^{-3/2} \epsilon_{B,-1}^{-3/2} E_{53}^{1/2} A_{11.7}^{-2} T_{50}^{1/2} \text{ Hz} \quad (1)$$

$$\nu_m(T) \sim 5.0 \times 10^{12} \zeta^{-1/2} \epsilon_{e,-2}^2 \epsilon_{B,-1}^{1/2} E_{53}^{-1/2} A_{11.7} \eta_2^2 T_{50}^{-1/2} \text{ Hz} \quad (2)$$

$$F_{\nu,max}(T) \sim 95 d^{-2} \zeta^2 \epsilon_{B,-1}^{1/2} E_{53} A_{11.7}^{1/2} \eta_2^{-1} T_{50}^{-1} \text{ Jy} \quad (3)$$

where $\epsilon_{B,-1} = \epsilon_B/10^{-1}$, $\epsilon_{e,-2} = \epsilon_e/10^{-2}$, $\eta_2 = \eta/100$, $d = d_L(z)/(2 \times 10^{28} \text{ cm})$, $d_L(z)$ is the luminosity distance of the burst, and $d_L(1) \sim 2 \times 10^{28} \text{ cm}$ for the standard cosmological parameters ($\Omega_m = 0.3$, $\Omega_\Lambda = 0.7$ and $h = 0.7$),

3. Self-absorption

In a stellar wind the external density at the initial interaction with the shell is much larger than in the typical ISM environment, hence the cooling frequency ν_c is lower than the typical peak frequency ν_m , and the synchrotron self-absorption (SA) frequency ν_a can be much higher than ν_m : $\nu_c(T) < \nu_m(T) < \nu_a(T)$. As suggested by some recent work (Zhang, Kobayashi & Mészáros 2003; Kumar & Panaiteescu 2003; Coburn & Boggs 2003), the fireball ejecta could be highly magnetized. In such cases the condition $\epsilon_e/\epsilon_B \ll 1$ can lead to a Compton parameter $Y \ll 1$ and the inverse Compton process is not important for electron cooling (the opposite case $Y \gg 1$ where inverse Compton is important is discussed below). A consequence of the dominance of the synchrotron process is that self-absorption suppresses the emission at frequencies lower than the SA frequency ν_a , and prevents the

electrons from cooling down to the Lorentz factor γ_c corresponding to the cooling frequency ν_c . The suppressed radiation energy is partly redistributed among the electrons, and results in a distinctive hump in the spectrum of the reverse shock emission.

The reverse shock injects accelerated electrons with a power law distribution of energies $N(\gamma)d\gamma \propto \gamma^{-p}d\gamma$ ($\gamma \geq \gamma_m$). The energy deposited in electrons with Lorentz factors between γ_m and γ_a is $E_e \sim (p-1)N_t\Gamma\gamma_m m_e c^2/(p-2)$ where N_t is the number of electrons in the shell, γ_a is the Lorentz factor corresponding to the SA frequency, m_e is the electron mass, and we assumed $p > 2$ and $\gamma_a \gg \gamma_m$ (so E_e is essentially the total energy of the electrons). This energy is redistributed among the electrons and photons in the optically thick regime within a timescale comparable to the cooling time (Ghisellini & Svensson 1989). Since the reverse shock is in the fast cooling regime ($\gamma_c < \gamma_m < \gamma_a$), the electrons have time enough to redistribute the energy. In a dynamical time, the energy E_e is radiated as photons around ν_a . Assuming $p = 3$, the flux at ν_a is given by

$$F_{\nu_a}(T) \sim \frac{1}{4\pi d_L^2} \frac{E_e}{\nu_a T} \sim \frac{2(\nu_c \nu_m)^{1/2}}{\nu_a} F_{\nu,max}. \quad (4)$$

A simple estimate of the maximal self-absorption flux is given by a black body flux with the reverse shock temperature (e.g. Sari & Piran 1999; Chevalier & Li 2000). We write this as $F_{\nu_a}^{bb} = 2\pi(1+z)^3 \nu_a^2 m_e \Gamma \gamma_a (R_\perp/d_L)^2$ where $R_\perp \sim 2\Gamma c T/(1+z)$ is the observed size of the shell. Using the equality $F_{\nu_a}^{bb} \sim F_{\nu_a}$, we obtain the SA frequency

$$\nu_a(T) \sim 8.1 \times 10^{13} \zeta^{-3/14} \epsilon_{e,-2}^{2/7} \epsilon_{B,-1}^{1/14} A_{11.7}^{2/7} E_{53}^{1/14} T_{50}^{-11/14} \text{ Hz.} \quad (5)$$

The SA frequency can also be determined by requiring that the electron synchrotron cooling rate and its heating rate (through absorption) are equal at γ_a . The cross section for the synchrotron absorption process is given by $\sigma_s \sim \gamma^{-5} r_e r_L$ (e.g. Ghisellini & Svensson 1991) where $r_e = q_e^2/m_e c^2$ and $r_L = m_e c^2/q_e B$ are the classical electron radius and the Larmor radius, q_e is the charge of an electron, $B = (32\pi\epsilon_B\Gamma^2\rho c^2)^{1/2}$ is the comoving magnetic field strength behind the shock. Using this cross section and the photon flux determined by eq. (4), we can evaluate the heating rate, while the cooling rate is given by the synchrotron power of an electron. Equating these two rates, we can reproduce eq. (5).

Using the method of Kobayashi & Zhang (2003b), we can obtain the scalings at $t < t_\times$ of the spectral quantities $\nu_c \propto t$, $\nu_m \propto t^{-1}$, $\nu_a \propto t^{-5/7}$, $F_{\nu,max} \propto t^0$. Although ν_c itself is not observed, as a result of the self-absorption, the flux at $\nu \gtrsim \nu_a$ can be still estimated from these scalings, because the electron distribution N_e producing some observed frequency ν (say in the K-band $\nu_K > \nu_a$) (and frequencies above this) is determined by the distribution of injected electrons at the shock, and by the synchrotron radiation cooling. Therefore, even though the flux at ν_a has a hump which was previously unaccounted

for, we can apply the conventional synchrotron model to estimate the light curve at a frequency $\nu \gtrsim \nu_a$. The optical/IR luminosity initially increases as $\sim (\nu/\nu_a)^2 F_{\nu_a} \propto t^{15/7}$. When the SA frequency passes through the observation band ν_{obs} at t_a , the flux reaches a peak of $F_{\nu_{obs}}(t_a) \sim 2(\nu_m \nu_c)^{1/2} F_{\nu, max} / \nu_{obs}$ and then it rapidly decreases by a factor of $\mathcal{R} \sim 2[\nu_{obs}/\nu_m(t_a)]^{(p-2)/2}$. The time of the absorption peak passage through the K-band (t_a), the peak flux ($F_{\nu_K}(t_a)$) and the peak flux contrast (\mathcal{R}) relative to the subsequent power-law decay value are given by

$$t_a \sim 20 \zeta^{-3/10} \epsilon_{e,-2}^{2/5} \epsilon_{B,-1}^{1/10} A_{11.7}^{2/5} E_{53}^{1/10} T_{50}^{-1/10} \nu_{obs,14.2}^{-7/5} \text{ sec}, \quad (6)$$

$$F_{\nu_K}(t_a) \sim 1 d^{-2} \zeta \epsilon_{e,-2} E_{53} T_{50}^{-1} \nu_{obs,14.2}^{-1} \text{ Jy}, \quad (7)$$

$$\mathcal{R} \sim 7 \zeta^{1/10} \epsilon_{e,-2}^{-4/5} \epsilon_{B,-1}^{-1/5} A_{11.7}^{-3/10} E_{53}^{3/10} \eta_2^{-1} T_{50}^{-3/10} \nu_{obs,14.2}^{-1/5} \quad (8)$$

where $\nu_{obs,14.2} = \nu_{obs}/(1.6 \times 10^{14} \text{ Hz})$ and $p = 3$ was assumed. At this turnover, a drastic color change from blue to red is expected (see fig 1). Since in the optically thick limit the polarization is to zero for a quasi-thermal spectrum, the shocked shell can emit polarized photons only above the turnover. If the turnover ($t_a, F_{\nu_K}(t_a)$) is observed, we can constrain the mass loss rate A . This assumes that redshift z has been measured, and that the explosion energy E of the GRB is determined, e.g. from late time bolometric afterglow observations. From the peak flux (eq. (7)), the equipartition parameter ϵ_e can be determined, while the peak time (eq. (6)) gives a constraint on the mass loss rate A , since the dependence on the other unknown parameter ϵ_B is weak.

After the optical/IR reverse shock emission drops to the level expected from the usual synchrotron model, the flux slowly decreases as $\sim (\nu_m/\nu_c)^{-1/2} (\nu/\nu_m)^{-p/2} F_{\nu, max} \sim t^{-(p-2)/2}$. Beyond a timescale comparable to the burst duration T , the optical/IR emission fades rapidly, because no further electrons are being shocked in the shell (allowing the initially weaker but longer lasting forward shock component to gradually dominate). The angular time delay effect prevents the abrupt disappearance of the reverse component, whose flux decreases steeply as $\sim t^{-(p+4)/2}$ (Kobayashi & Zhang 2003b). No color change is expected around this break. The flux value at this break for $p = 3$ is given by

$$F_{\nu_K}(T) \sim 0.1 d^{-2} \zeta^{3/4} \epsilon_{e,-2}^{2} \epsilon_{B,-1}^{1/4} A_{11.7}^{1/2} E_{53}^{3/4} \eta_2 T_{50}^{-5/4} \nu_{obs,14.2}^{-3/2} \text{ Jy}. \quad (9)$$

These two breaks are schematically shown in Fig. 2, the sharpness of the transition being an idealization; in reality these would appear rounded. In our treatment, we have ignored pair formation ahead of the blast wave, e.g. Beloborodov (2002), which may modify the forward shock spectrum and light curve.

The above discussion assumed $\epsilon_e/\epsilon_B \ll 1$ and $Y < 1$. However, if the magnetic energy density is sufficiently low that $\epsilon_e/\epsilon_B \gg 1$, the inverse Compton (IC) process can affect the

observed spectrum and the light curve. Although the fraction of photons scattered to higher energies is small, they carry away a majority of the electron energy. The energy available for the synchrotron process is reduced from the injected energy E_e by a factor of $(1 + Y)$ where $Y = (\epsilon_e/\epsilon_B)^{1/2}$ is the Compton Y parameter (e.g. Zhang & Mészáros 2001). The IC process enhances the electron cooling, so ν_c is smaller by a factor of $(1 + Y)^2$ than its previous (synchrotron only) value. The thermal bump is shifted to a lower frequency, becoming less prominent or even disappearing. As a consequence of the IC cooling, the flux at ν_a becomes smaller by a factor of $\sim (1 + Y)$ than the value given by eq. (4). If ν_a is shifted below ν_m , most of the energy available for the synchrotron process is radiated between ν_a and ν_m . The flux at ν_a is reduced from eq. (4) by a factor of $\sim (1 + Y)(\gamma_m/\gamma_a) \sim (1 + Y)(\nu_m/\nu_a)^{1/2}$. By equalizing the flux at ν_a and the black body flux at the reverse shock characteristic temperature $\gamma_a \propto \nu_a^{1/2}$, we can obtain the SA frequency. For the same parameters as for eq. (4) but taking $\epsilon_{e,-1} = \epsilon_e/10^{-1}$ and $\epsilon_{B,-3} = \epsilon_B/10^{-3}$, we get $\nu_a(T) \sim 5.8 \times 10^{13} \zeta^{-3/14} \epsilon_{e,-1}^{1/7} \epsilon_{B,-3}^{3/14} A_{11.7}^{2/7} E_{53}^{1/14} T_{50}^{-11/14}$ Hz and $\nu_m(T) \sim 5.0 \times 10^{13} \zeta^{-1/2} \epsilon_{e,-1}^2 \epsilon_{B,-3}^{1/2} E_{53}^{-1/2} A_{11.7} \eta_2^2 T_{50}^{-1/2}$ Hz. To produce a significant bump, the SA frequency ν_a should be much higher than the typical frequency ν_m . When $\nu_a \lesssim \nu_m$, as in this case, the contrast \mathcal{R} is $\lesssim 2$ and the bump practically disappears. The optical/IR light curve initially increases as $\sim (\nu/\nu_a)^{5/2} F_{\nu_a} \propto t^{5/2}$, and after ν_a crosses the observation band, it decreases as $t^{-(p-2)/2}$. The transition is expected to be gradual and smooth.

Since at the shock crossing time the forward and reverse shocked regions have roughly comparable energy, the νF_{ν} peaks of the synchrotron emissions reach roughly similar levels. Assuming that the characteristic reverse shock IC frequency $\nu_{a,IC} \sim \gamma_a^2 \nu_a$ is close to the typical (peak) frequency of the forward shock synchrotron emission, we can infer that in the case of $Y \ll 1$ the reverse shock IC component is generally masked by the forward shock synchrotron emission, whereas in the case of $Y \gg 1$ the reverse shock IC peak sticks out above the forward shock synchrotron peak. Therefore, if the fireball is not strongly magnetized ($Y \gtrsim 1$), a prompt X-ray flare is expected from the reverse shock. The characteristic photon energy and the flux at this frequency are $\nu_{a,IC}(T) \sim 20 \zeta^{-3/7} \epsilon_{e,-1}^{2/7} \epsilon_{B,-3}^{-1/14} E_{53}^{1/7} A_{11.7}^{1/14} T_{50}^{-4/7}$ keV and $F_{\nu_{a,IC}}(T) \sim 1 d^{-2} \zeta^{31/14} \epsilon_{e,-1}^{9/7} \epsilon_{B,-3}^{3/7} E_{53}^{9/14} A_{11.7}^{15/14} T_{50}^{-17/14}$ mJy, respectively. The typical duration of this X-ray flare at $\nu \gtrsim \nu_{a,IC}$ is of order the shock crossing time $t_{\times} \sim T = 50 T_{50}$ s. After the reverse shock crosses the shell, electrons are no longer heated and the (on-axis) synchrotron flux at $\nu > \nu_a(T)$ drops, as does the the IC emission at $\nu > \nu_{a,IC}$, and one starts to observe high latitude emission. The X-ray emission from the reverse shock decays as $t^{-(p+4)/2}$, whereas the forward shock emission decays $\propto t^{-(3p-2)/4}$. Thus the slower decaying forward shock component gradually starts to dominate.

4. Dense ISM in Early Galaxies

We consider a specific model in which the ISM density of early galaxies scales with redshift as $n \sim (1+z)^4 n_0 \text{ cm}^{-3}$ (e.g. Ciardi & Loeb, 2000). For this model (or in general for cases where the ISM density is much larger than the typical $n_0 \sim 1 \text{ proton cm}^{-3}$ assumed at $z = 0$), a discussion similar to that of the previous section can also lead to a bump in the reverse shock spectrum and in the optical/IR light curve.

The critical Lorentz factor classifying the evolution of the reverse shock is given by (e.g. Kobayashi 2000) $\eta'_{cr} \sim 90 n_0^{-1/8} \zeta_6^{-1/8} E_{53}^{1/8} T_{2.2}^{-3/8}$ where $\zeta_6 = (1+z)/6$ and $T_{2.2} = T/150 \text{ sec}$. A large fraction of GRBs would be expected to be classified as thick shell cases. For the thick shell, the spectral quantities are given by (Kobayashi & Zhang 2003a) $\nu_c(T) \sim 2.0 \times 10^{11} n_0^{-1} \zeta_6^{-9/2} \epsilon_{B,-1}^{-3/2} E_{53}^{-1/2} T_{2.2}^{-1/2} \text{ Hz}$, $\nu_m(T) \sim 7.2 \times 10^{11} n_0^{1/2} \zeta_6 \epsilon_{e,-2}^2 \epsilon_{B,-1}^{1/2} \eta_2^2 \text{ Hz}$ and $F_{\nu,max}(T) \sim 27 n_0^{1/4} D^{-2} \zeta_6^{11/4} \epsilon_{B,-1}^{1/2} E_{53}^{5/4} \eta_2^{-1} T_{2.2}^{-3/4} \text{ Jy}$, where $D = d_L(z)/(1.5 \times 10^{29} \text{ cm})$ is the normalized luminosity distance and $D(z=5) = 1$. From equating $F_{\nu_a}^{bb} \sim F_{\nu_a}$, we obtain $\nu_a(T) \sim 3.7 \times 10^{13} n_0^{1/7} \zeta_6^{3/14} \epsilon_{e,-2}^{2/7} \epsilon_{B,-1}^{1/14} E_{53}^{3/14} T_{2.2}^{-9/14} \text{ Hz}$. Using the scalings by Kobayashi (2000), it is possible to show that ν_a behaves as $t^{-3/7}$ during the shock crossing. The optical/IR light curve initially increases as $\sim (\nu/\nu_a)^2 F_{\nu_a} \propto t^{9/7}$. When ν_a passes through the K-band at $t_a \sim 5 n_0^{1/3} \zeta_6^{1/2} \epsilon_{e,-2}^{2/3} \epsilon_{B,-1}^{1/6} E_{53}^{1/2} T_{2.2}^{-1/2} \nu_{obs,14.2}^{-7/3} \text{ sec}$, the flux reaches a peak of $F_{\nu_K}(t_a) \sim 0.1 D^{-2} \zeta_6 \epsilon_{e,-2} E_{53} T_{2.2}^{-1} \nu_{obs,14.2}^{-1} \text{ Jy}$, and then it rapidly decreases by a (bump contrast) factor of $\mathcal{R} \sim 30 n_0^{-1/4} \zeta_6^{-1/2} \epsilon_{e,-2}^{-1} \epsilon_{B,-1}^{-1/4} \eta_2^{-1} \nu_{obs,14.2}^{1/2} (p=3)$. After the emission drops to the level expected from the usual synchrotron model, the flux keeps a constant level, and then it rapidly fades as $t^{-(p+4)/2}$ after a time comparable to the burst duration.

5. Discussion and Conclusions

We have analyzed the prompt afterglow emission from the reverse shocks of GRBs which occur in dense environments, such as the stellar wind produced by their massive progenitor, or a dense ISM such as might be expected in early galaxies. Usually in the fast cooling case, the νF_{ν} flux is normalized at the typical frequency ν_m by using the energy ejected into electrons. However, here we point out that if the synchrotron self absorption frequency ν_a is higher than the typical frequency ν_m (and ν_c), this usual prescription should be inapplicable for estimating the flux at and below ν_a . Such conditions can occur in the reverse shock of a highly magnetized fireball in a dense environment. The radiation flux suppressed by the self absorption effect is redistributed among the electrons and photons in the optically thick regime, and most of it is emitted at $\sim \nu_a$ in a dynamical time. As a result, the self-absorption frequency is different and scales differently with the shock parameters, and the flux at the

self-absorption frequency shows a bump which is a factor $2(\nu_a/\nu_m)^{(p-2)/2}$ (\sim several) above the usual power law flux estimate for typical parameters. The flux well above ν_a is the same as before, but the flux below ν_a is larger by the same factor $2(\nu_a/\nu_m)^{(p-2)/2}$. This results in a new type of temporal behavior for the prompt optical flash of afterglows from fireballs in dense (e.g. wind or early galaxy) environments. These new features will be prominent when the inverse Compton process is not important for electron cooling, i.e. for ejecta with $\epsilon_e/\epsilon_B \ll 1$. This may be the case in fireball ejecta which are highly magnetized, as suggested by some recent studies. If, on the other hand, the burst occurs in a dense environment and such features are absent, this may be an indication that $\epsilon_e/\epsilon_B \gg 1$, and in this case a prompt reverse shock X-ray flare is expected, which for a brief time dominates the forward shock but decays faster than it.

Massive stars appear implicated in producing long gamma-ray bursts (as seen from the detection of a supernova associated with GRB 030329, e.g., Stanek et al 2003). Wind mass loss is expected from such stars previous to the GRB explosion, but snapshot fits to forward shock late emission (e.g., Panaitescu & Kumar, 2002) are compatible with such wind mass loss in only a handful of cases. In general the parameters of stellar winds are poorly known, and the uncertainties are further increased at high redshifts, where massive stars are expected to be metal poor. For this reason, signatures of a wind mass loss or a dense environment would be extremely valuable, both for GRB astrophysics and for tracing the properties of star formation at high redshifts. The prompt optical flashes expected after tens of seconds from the reverse shock in a dense environment would give characteristic signatures in the spectral and temporal behavior. These may help to test for the presence of winds and constrain the wind mass loss, in moderate redshift environment, or alternatively, at high redshifts they may provide evidence for a denser ISM than at low redshifts. In such winds or dense ISM the spectra and light curve time behavior can also give constraints on the strength of the magnetic field in the ejecta. Large numbers of prompt X-ray detections with future missions such as *Swift*, complemented by ground-based follow-ups, should be able to test for such wind or dense ISM signatures and trace any changes with redshifts, if they exist, thus constraining the GRB environment as well as the radiation mechanisms.

We thank M. Rees, J. Granot, A. Beloborodov and the referee for valuable comments. This work is supported by NASA NAG5-13286 and the Pennsylvania State University Center for Gravitational Wave Physics, funded by NSF under cooperative agreement PHY 01-14375.

REFERENCES

Beloborodov, A. M. 2002, *ApJ*, 565, 808.
Chevalier,R.A. & Li,Z.Y. 1999, *ApJ*, 520, L29.
Chevalier,R.A. & Li,Z.Y. 2000, *ApJ*, 536, 195.
Ciardi, B. & Loeb, A, 2000, *ApJ*, 540, 687.
Coburn,W. & Boggs, S.E. 2003, *Nature*, 423, 415.
Frail, D.A. et al. 2001, *ApJ*, 562, L55.
Ghisellini,G. & Svensson,R. 1989, in NATO ASI Series Proc, Physical processes in hot cosmic plasmas, p. 395.
Ghisellini,G. & Svensson,R. 1991, *MNRAS*, 252, 313.
Kobayashi,S. 2000, *ApJ*, 545, 807.
Kobayashi,S, Piran,T. & Sari,R. 1997, *ApJ*, 490, 92.
Kobayashi,S & Zhang,B. 2003a, *ApJ*, 582, L75.
Kobayashi,S & Zhang,B. 2003b, *ApJ* in press, astro-ph/0304086.
Kumar,P. & Panaiteescu,A. 2003, astro-ph/0305446.
Li,Z.Y. & Chevalier,R.A. 2003, *ApJ*, 589, L69.
Lithwick,Y & Sari, R. 2001, *ApJ*, 555, 540.
Panaiteescu,A. & Kumar, P. 2002, *ApJ*, 571, 779.
Sari,R. & Piran,T. 1995, *ApJ*, 455, L143.
Sari,R. & Piran,T. 1999, *ApJ*, 517, L109.
Sari,R., Piran,T. & Narayan,R. 1998, *ApJ*, 497, L17.
Stanek,K.Z. et al. 2003, *ApJ*, 591, L17.
Zhang,B., Kobayashi,S. & Mészáros,P. 2003, *ApJ*, 595, 950.
Zhang,B. & Mészáros , P. 2001, *ApJ*, 559, 110.

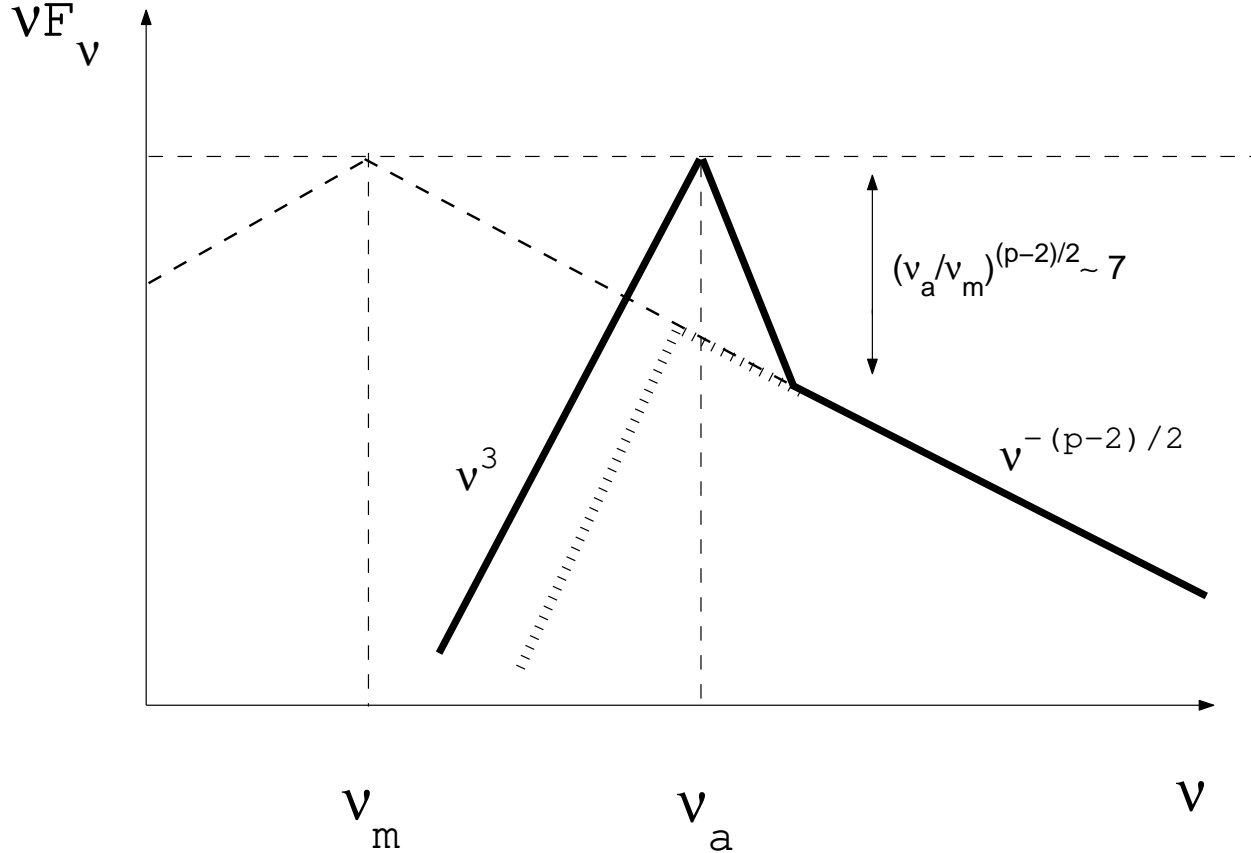


Fig. 1.— Reverse shock spectrum in a dense environment or wind when synchrotron losses dominate: with self-absorption (thick solid) and without self-absorption (thin dashed). The schematic self-absorption maximum would appear as a rounded thermal peak. The previous self-absorbed flux estimate is shown by hashed lines. The correction factor $2(\nu_a/\nu_c)^{(p-2)/2} \propto t^{(p-2)/7}$ is slightly larger at later times ($t \sim t_x$), the value of ~ 7 is evaluated at t_a for typical parameters.

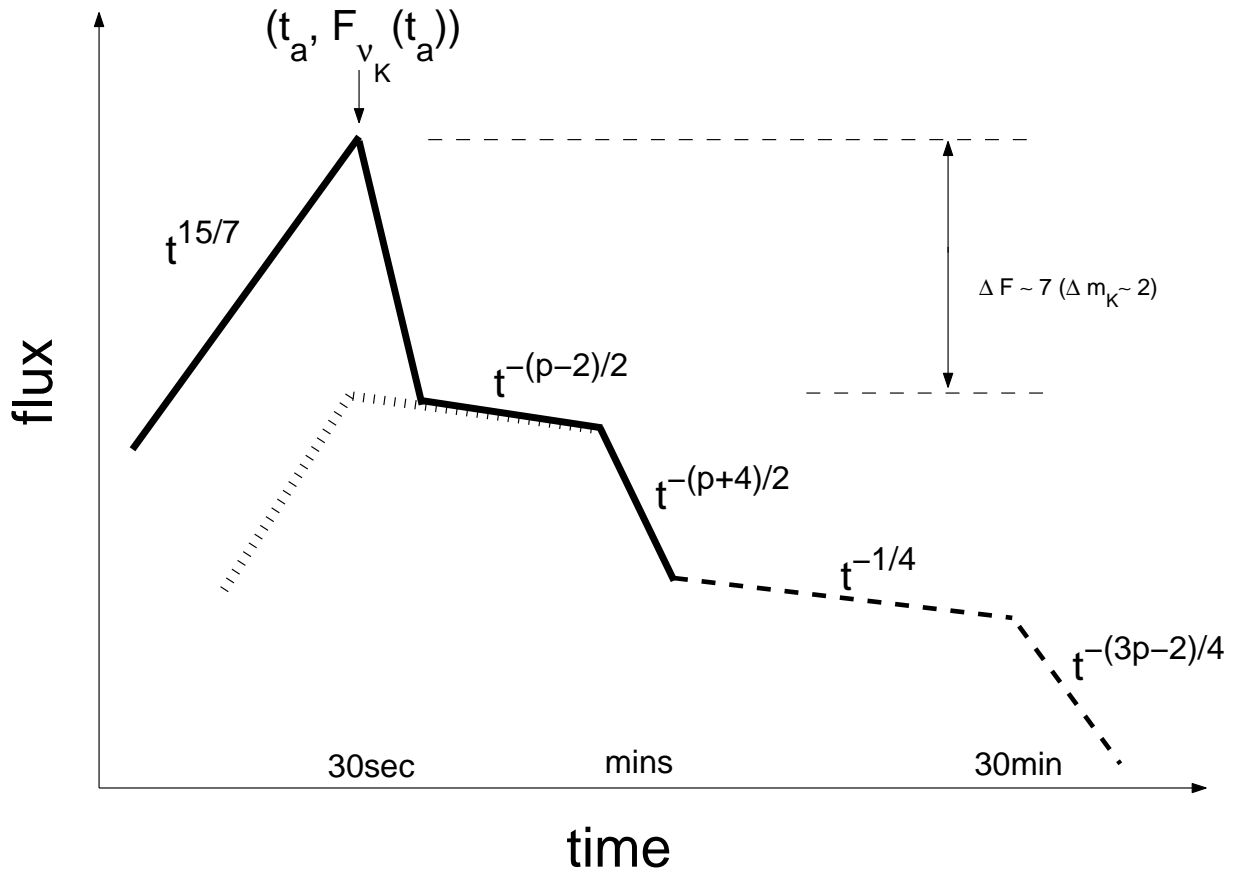


Fig. 2.— Schematic optical light curve for a synchrotron dominated fireball in a dense environment or wind: reverse shock emission (solid) and forward shock emission (dashed). The hashed line shows a previous estimate. Time scales are rough estimates for the typical parameters.